Adsorption of a multicomponent rhamnolipid surfactant to soil

Noordman, Wouter H.; Brusseau, Mark L.; Janssen, Dick

Published in:
Environmental Science & Technology

DOI:
10.1021/es9909982

Environ. Sci. Technol. **2000**, *34,* 832−838

Adsorption of a Multicomponent Rhamnolipid Surfactant to Soil

WOUTER H. NOORDMAN,[†] MARK L. BRUSSEAU,[‡] AND DICK B. JANSSEN*,[†]

Department of Biochemistry, Groningen Biomolecular Sciences and Biotechnology Institute, University of Groningen, Nijenborgh 4, 9747 AG Groningen, The Netherlands, and Soil, Water and Environmental Science Department, University of Arizona, Tucson, Arizona 85721

The adsorption of rhamnolipid, a multicomponent biosurfactant with potential application in soil remediation, to two sandy soils was investigated using batch and column studies. The surfactant mixture contained six anionic components differing in lipid chain length and number of rhamnose moieties. Batch adsorption experiments indicated that the overall adsorption isotherms of total surfactant and of the individual components leveled off above a concentration at which micelles were formed. Column experiments showed that the retardation factors for the total surfactant and for the individual components decreased with increasing influent concentration. Extended tailing was observed in the distal portion of the surfactant breakthrough curve. The concentration-dependent retardation factors and the extended tailing are in accordance with the nonlinear (concave) adsorption isotherms found in the batch adsorption studies. The more hydrophobic rhamnolipid components were preferentially adsorbed, but adsorption was not correlated with the organic carbon content of the soil. This suggests that adsorption of rhamnolipid to soil is not a partitioning process but mainly an interfacial adsorption process.

Introduction

The understanding of surfactant adsorption is of importance for the application of surfactants for enhanced oil recovery (*1, 2*) and for surfactant-enhanced soil remediation (*3*−*6*). Adsorption of surfactants is detrimental for these applications as it results in surfactant loss and reduced surfactant mobility. Furthermore, adsorption of surfactants may create new adsorption sites for hydrophobic compounds (*7*). Many commercially available surfactants such as linear alkylbenzenesulfonates (*8*) and alcohol ethoxylates (*9*) consist of multiple components. Natural surfactants also often are mixtures (*10*−*14*). Multicomponent surfactants may change in composition during adsorption and transport, which can result in altered surface active properties (*2*). Insight into the adsorption behavior of multicomponent surfactants thus is needed for understanding surfactant transport and for optimal design of surfactant mixtures (*2, 4*).

Rhamnolipid is a bacterial biosurfactant produced by several *Pseudomonas* species as a mixture of α-L-rhamnopyranosyl-β-hydroxyalkanoyl-β-hydroxyalkanoate and 2-*O*-α-L-rhamnopyranosyl-α-L-rhamnopyranosyl-β-hydroxyalkanoyl-β-hydroxyalkanoate species (*13, 15, 16*). These biosurfactants resemble synthetic gemini surfactants because they contain two covalently linked headgroups (a nonionic (di)rhamnopyranosyl and an anionic carboxylate headgroup) and two tails (*17*). Rhamnolipid has potential for application in foods (*18*), use as pest-control agent (*16, 19*), as a source of rhamnose (*20*), and for the remediation of soils contaminated with sparingly soluble organic compounds and heavy metals (*5, 6, 15, 21*). Favorable properties of rhamnolipid for application in soil remediation include the relatively low adsorption to soil and the solubilization characteristics, which are similar to those of synthetic surfactants (*5*).

The factors that determine rhamnolipid adsorption to soil have not been elucidated, and the occurrence of preferential adsorption of specific components has not been investigated. For application of rhamnolipid as well as of other multicomponent surfactants in situations where adsorption occurs, knowledge of the factors that determine surfactant adsorption and of preferential adsorption of individual components is indispensable. Therefore, we investigated the adsorption of the surfactant mixture and of the individual components to soil using batch adsorption and column experiments. Two frequently used representative sandy soils, the Borden material and Eustis soil, were selected for this study (*5, 22*−*24*).

Materials and Methods

Soils and Solutions. The Borden material is a sandy subsoil collected at the Canadian Air Force base in Borden, Ontario, Canada (*23*). This material consisted primarily of sand (>99%) and had an organic carbon content of 0.03%. Eustis soil is a sandy surface soil from Florida, U.S.A. (*22*) that consisted of 95.1% sand, 2.2% silt; 2.7% clay, and 0.27% organic carbon. Soils were air-dried and sieved (<2 mm) prior to use. In all experiments, a background electrolyte solution was used which contained 10 mM KNO_3, 10 mM Tris-HCl, pH 7.0, and 3 mM NaN_3 (to suppress microbial activity) in MilliQ water.

Rhamnolipid. Rhamnolipid was produced by *Pseudomonas aeruginosa* UG2 (*15*) and isolated by consecutive steps of acid precipitation and dissolution in aqueous $NaHCO_3$ solution (*21*). Acid-precipitated rhamnolipid was purified by column chromatography over Sephadex LH20 with methanol as the eluent. Fractions were analyzed for rhamnolipid content and purity by TLC. Pooled fractions were evaporated to dryness and dissolved in water. The pH was adjusted to 7.0 using $NaHCO_3$. The rhamnolipid concentration in this stock solution was determined using the 6-deoxyhexose assay with L-rhamnose as a standard (*25*). For this mixture, an average molecular weight of 588 and a rhamnose content of 0.45 (w/w) were calculated using the composition of the mixture as determined with HPLC. About 1.4 g of purified rhamnolipid was isolated per liter of culture medium. This multicomponent surfactant mixture was used in all experiments.

Batch Adsorption Experiments. Adsorption of rhamnolipid to soil was measured in a 1:2 (w/v) soil:solution ratio in 8 mL Pyrex tubes that were closed with aluminum coated septa. After 2−7 days of end-over-end rotation (1.4 rpm, room temperature), the incubation vessels were centrifuged at 3000 rpm for 20 min, and subsequently the clear supernatant was analyzed for the concentration of total aqueous surfactant (C, μM) by surface tension measurements or, in a separate experiment, for the individual C20 components (C, μM) by HPLC. The adsorbed concentration of total surfactant or

* Corresponding author phone: +31-50 363 4209; fax: +31-50 363 4165; e-mail: D.B.Janssen@chem.rug.nl.
[†] University of Groningen.
[‡] University of Arizona.

10.1021/es9909982 CCC: $19.00
Published on Web 02/03/2000

TABLE 1. Properties of the Rhamnolipid Produced by *P. aeruginosa* UG2

	total surfactant	C18RL2	C18RL1	C20RL2	C22:1RL2	C20RL1	C22RL2
molecular weight	588[a]	622	476	650	776	504	678
mole fraction in mixture		0.06	0.11	0.49	0.02	0.28	0.03
HPLC retention time (min)		3.5	6	7	9	12	14
MS major ions (M + TFA[b] − 1)		735	589	763	789	617	791
MS major ions (M − 1)		621		649			

[a] Average molecular weight. [b] Trifluoroacetic acid, a component of the eluens (molecular weight = 114).

individual components (S, μmol/kg) was determined from the difference in the rhamnolipid concentration in the aqueous phase before and after adsorption. To determine the mass balances, the amount of adsorbed rhamnolipid was measured after removal of the aqueous phase by extracting several soil pellets three times with methanol. These mass balance checks revealed a total rhamnolipid recovery of 92−124%. Five initial concentrations (85−1275 μM), in triplicate, were used to determine the isotherms of total surfactant. Nineteen initial concentrations (2−2000 μM) were used to determine the isotherms for the individual C_{20} components.

One batch adsorption experiment was performed on a larger scale by contacting 37.5 g of Borden soil and 75 mL of 700 μM rhamnolipid solution. After equilibration for 24 h, the aqueous phase was removed, analyzed by HPLC, and concentrated by lyophilization. The cmc of this concentrated mixture was determined using surface tension measurements. All adsorption experiments were performed at 22 ± 2 °C.

Column Experiments. The experimental setup for the column studies was described previously by Noordman et al. (*5*). A stainless steel column of 7.0 cm length and 2.2 cm i.d. was used. The bulk density (ρ) and porosity (θ) were determined gravimetrically. Flow rates and pore water velocities used were 0.4 mL/min and 20 cm/h, respectively, for Borden material and 2 mL/min and 90 cm/h, respectively, for Eustis soil, unless specified otherwise. The experiments were performed at 22 ± 2 °C. Breakthrough of the conservative tracer pentafluorobenzoic acid was analyzed using a flow-through variable wavelength detector at 250 nm. For the experiments with rhamnolipid, the column effluent was directed to a fraction collector and analyzed for rhamnolipid using surface tension measurements or, in independent experiments, by HPLC. After the effluent concentration reached the concentration in the influent (C_0, 34 or 850 μM total rhamnolipid), elution was continued with a rhamnolipid-free solution. The experiments were continued until the effluent contained extremely low (surface tension > 69 mN/m) or no detectable amount of rhamnolipid.

The Peclet number for each column was determined by analysis of the breakthrough curve of the conservative tracer with a local equilibrium advective-dispersive transport model using nonlinear least squares optimization (*26*). The retardation factors (R) for total surfactant and for the components were determined from the area above the frontal limb of the breakthrough curves. Moment analysis revealed a total recovery of rhamnolipid of 96−116%.

Analytical Procedures. The surface tension of aqueous rhamnolipid solutions was measured using a du Nouy ring tensiometer (Fischer Scientific, model 21, Pittsburgh, PA). Surfactant concentrations were determined quantitatively by surface tension measurements after dilution to concentrations where the surface tension was linearly correlated with the logarithm of the aqueous concentration (1−20 μM total rhamnolipid, experimental error 5%). The surface tension analyses were calibrated with dilutions of the rhamnolipid stock solution. The surface tension of the electrolyte solution was higher than 70 mN/m.

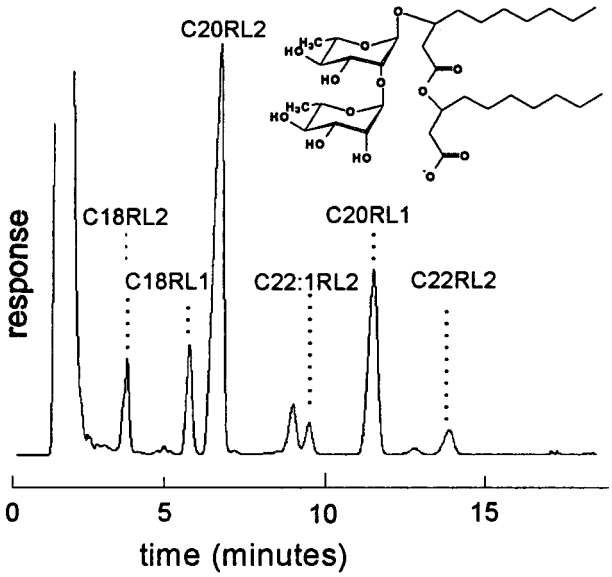

FIGURE 1. HPLC-ELSD chromatogram of rhamnolipid from *P. aeruginosa* UG2. Abbreviations denote components. The inset shows the structure of the main component (C20RL2).

Individual rhamnolipid components were analyzed by HPLC using a Merck AS 4000 autosampler, a Merck L-6200 pump, and a Chromsphere PAH 100 mm column (Chrompack, Bergen op Zoom, The Netherlands). Detection was done using an evaporative light scattering detector (ELSD, MARK III, Varex, Burtonsville, U.S.A.) (*9, 14, 27, 28*). Two sets of conditions were used. For the standard conditions, the mobile phase contained 55% acetonitrile, 45% water, and 0.03% trifluoroacetic acid (isocratic); the flow rate was 0.5 mL/min; the injection volume was 150 μL; the ELSD drift tube temperature was 100 °C; and the nebulizer flow was 1.5 L/min. For the analysis of samples with low rhamnolipid concentrations, the mobile phase contained 35% water, 45% acetonitrile, 20% methanol, and 0.03% trifluoroacetic acid (isocratic); the flow rate was 0.5 mL/min; the injection volume was 500 μL; the ELSD drift tube temperature was 80 °C; and the nebulizer flow was 1.0 L/min. Because pure components were not available, the mass fractions of the individual rhamnolipid species in the stock solution were determined from their respective relative peak areas at a total rhamnolipid concentration of 850 μM assuming that the ELSD response is directly related to the mass of compounds applied (*28*). The mass fractions thus obtained allowed calculation of the mole fractions of the components in the mixture, the rhamnose content, and the average molecular weight (Table 1). For several experiments (Figures 6 and 7), the total rhamnolipid concentration was calculated from the concentration of the individual components.

The lipid components of rhamnolipid where analyzed by GC-MS after hydrolysis and methylation of the total surfactant mixture (*29*). For the HPLC-MS analysis of the rhamnolipid produced by strain UG2, 50 nmol (50 μL of an aqueous solution containing 1 mM purified rhamnolipid) was sepa-

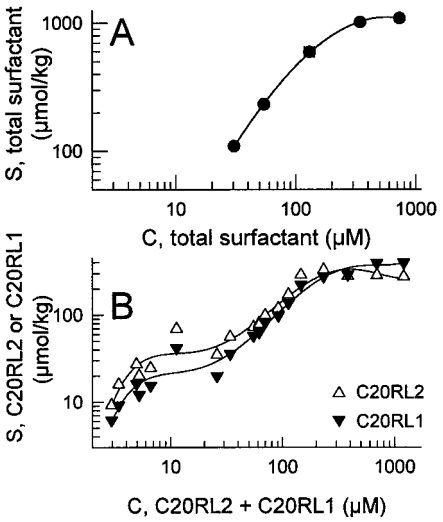

FIGURE 2. Adsorption isotherms of rhamnolipid on Borden soil. (A) Adsorption of total rhamnolipid (●). Error bars denote 1 SD and may be within symbol size. The *X*-axis gives the total aqueous surfactant concentration. (B) Adsorption of the individual components C20RL2 (△) and C20RL1 (▼). The total aqueous concentration of the C20 components is plotted on the *X*-axis.

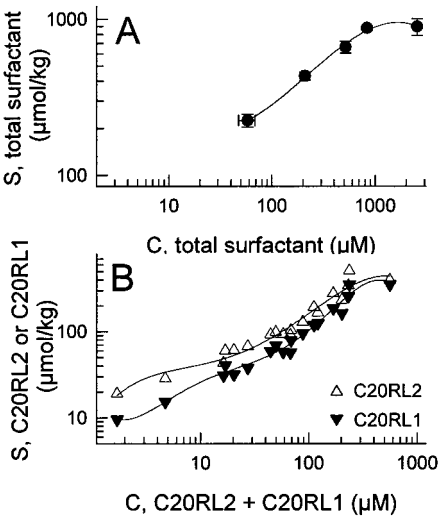

FIGURE 3. Adsorption isotherms of rhamnolipid on Eustis soil. Details are described in the legend of Figure 2.

rated by HPLC as described above. The HPLC eluate was directly introduced into a Nermag R 3010 triple quadrupole mass spectrometer operated in negative ion mode using an ionization potential of 3.5 kV and a nozzle potential of 70 V.

Results and Discussion

Analysis and Composition of Rhamnolipid. The rhamnolipid produced by *Pseudomonas aeruginosa* strain UG2 was analyzed by mass spectrometry to determine the composition of the mixture. GC-MS analysis of the methylated fatty acids of total rhamnolipid showed mass spectra corresponding to the methyl esters of β-hydroxydecanoic acid and β-hydroxydodecanoic acid. An HPLC-ELSD chromatogram of the surfactant showed six rhamnolipid components: C18RL2, C18RL1, C20RL2, C20RL1, C22:1RL2, and C22RL2 (Figure 1). The abbreviation C*x(:y)*RL*n* designates the individual component with *x* as the total number of carbon atoms in the lipid moieties, *y* as the number of unsaturated bonds in the lipid moieties, and *n* as the number of rhamnose groups. These components were identified by HPLC-MS (Table 1). The small peak that eluted between C20RL2 and C22:1RL2

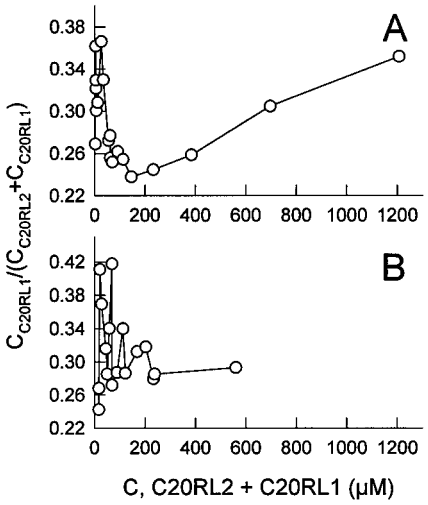

FIGURE 4. Preferential adsorption of rhamnolipid in the batch adsorption experiment with Borden material (A) and Eustis soil (B). The composition of the aqueous phase, expressed as the ratio of C20RL1 over total aqueous C20 compounds, is plotted against the aqueous concentration of C20 compounds.

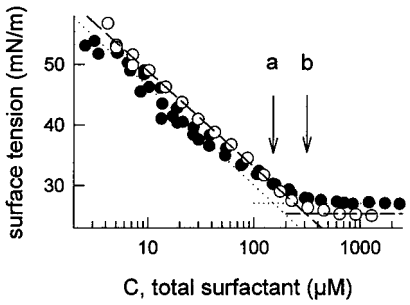

FIGURE 5. Determination of the cmc of the initial rhamnolipid mixture (●, dotted lines) and of the postadsorption mixture (○, dashed lines, details described in text) from the relation between the surface tension of the surfactant mixture and the aqueous concentration. The arrows indicate the cmc for the initial surfactant mixture (a) and for the postadsorption mixture (b) as calculated from the intercept of the regression lines of the supra- and sub-cmc data.

showed a large signal at a m/z of 777, which is the expected value for C21RL2. However, since a C11-lipid was not observed with GC-MS and the presence of odd-numbered lipids in rhamnolipid has never been reported, identification of this component as C21RL2 would need further investigation. The main component C20RL2 constituted almost 50 mol % of the mixture. The combined HPLC-MS and GC-MS analysis indicated that rhamnolipid produced by strain UG2 was a mixture of monorhamnolipids and dirhamnolipids, mainly containing β-hydroxydecanoic acid moieties, but also β-hydroxy-octanoic, -dodecenoic, and -dodecanoic acid moieties. This has also been found for other strains (*13*, *27*).

HPLC-ELSD was used to determine the concentration of the rhamnolipid components in subsequent experiments. When the standard set of experimental conditions was used, the concentrations of individual rhamnolipids could be determined in the range of 8−1700 μM with high accuracy (experimental error 3%). For lower concentrations, the use of a different eluent allowed operation of the ELSD at a lower nebulizer flow rate and drift tube temperature. This, together with a larger injection volume, increased the sensitivity of the analysis and allowed determination of individual components down to 1 μM with a maximal experimental error of 10% at the lowest concentration. The ELSD response was linear with the rhamnolipid concentration in the range of concentrations used. The HPLC-ELSD method provided a

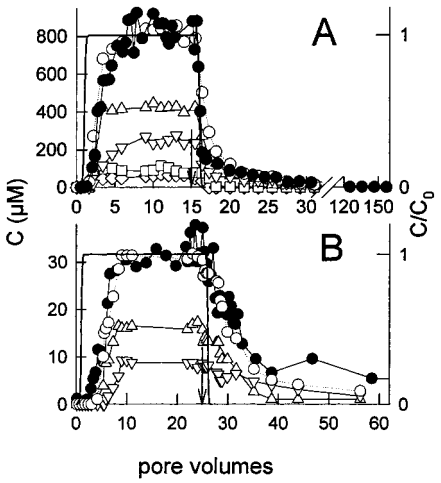

FIGURE 6. Breakthrough curve of rhamnolipid through Borden soil. From the time indicated by an arrow, elution was continued with a rhamnolipid-free solution. (A) C_0 = 850 μM; (B) C_0 = 34 μM. Symbols: (●) Total surfactant as determined by surface tension; (○) total surfactant as calculated from four of the individual components; (△) C20RL2; (▽) C20RL1; (◇) C18RL2; (□) C18RL1; (solid line, right *Y*-axis) PFBA.

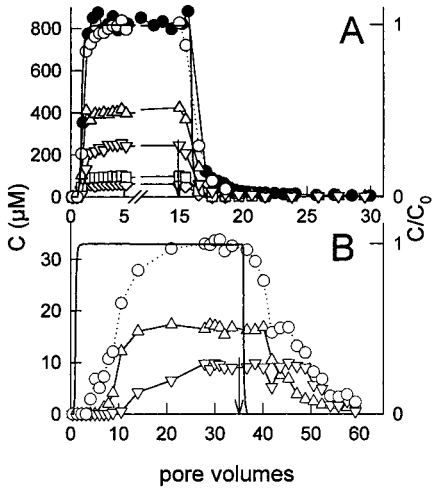

FIGURE 7. Breakthrough curve of rhamnolipid through Eustis soil. Details are described in the legend of Figure 6.

sensitive and accurate method to determine the aqueous concentrations of individual rhamnolipid components without need for prior derivatization.

Batch Adsorption Experiments. Adsorption isotherms were determined for the total surfactant and for the individual components using batch incubations with the Borden and Eustis soils (Figures 2 and 3). The isotherms were composed of three regions. Up to 40 μM C20 components (region I), the isotherms were a concave function of concentration. Especially for the Borden material, the adsorbed concentration of C20RL1 and C20RL2 in the first part of this region was rather high, indicating strong interactions between rhamnolipid and adsorption sites (Figure 2b). Subsequently, in region II, the adsorbed concentrations showed a more pronounced increase with increasing aqueous concentration, indicative of secondary interactions between adsorbed surfactants. The isotherms reached a plateau value at concentrations of approximately 300 μM C20 components (region III). Region I and II could not as well be distinguished with the Eustis soil as with the Borden material.

The composition of the surfactant remaining in solution changed due to preferential adsorption of the hydrophobic components. For instance, the mole fractions of C18RL2, C18RL1, C20RL2, C20RL1, C22:1RL2, and C22RL2 in the mixture that remained in solution after adsorption to Borden soil at an aqueous surfactant concentration of 404 μM were 0.13, 0.11, 0.62, 0.13, 0.01, and 0.01, respectively. From a comparison with the values for the initial mixture (Table 1), it is apparent that the aqueous phase was enriched with the hydrophilic C18 components and depleted of the relatively hydrophobic components C20RL1, C22:1RL2, and C22RL2.

The concentration-dependence of the preferential adsorption of the hydrophobic components was examined by plotting the ratio of aqueous C20RL1 over total aqueous C20 components as a function of the total aqueous concentration of C20 components (Figure 4). A decrease in this ratio indicates preferential adsorption of the hydrophobic component C20RL1. For the Borden material, the ratio was scattered around the initial value when the concentrations of C20 components were below 40 μM, indicating that preferential adsorption was not detected in region I (Figure 4A). In region II, this ratio was lower (e.g. 0.24 at 150 μM, Figure 4A) than with the initial mixture (0.34, Table 1). In the third adsorption region, the ratio of aqueous C20RL1 over total aqueous C20 components increased with increasing aqueous surfactant concentration and finally approached the initial value. This is due to accumulation in the aqueous phase of all surfactant that is added after the plateau is reached. For the Eustis soil, the ratio was lower than the initial value for virtually all concentrations (Figure 4B). These results show that the composition of the surfactant in the aqueous phase was influenced by preferential adsorption of the more hydrophobic components.

To determine if the onset of micellization was the cause of surfactant adsorption reaching a plateau, the cmc was determined for a rhamnolipid mixture that remained in solution after adsorption to Borden soil. After adsorption, the aqueous rhamnolipid concentration was 404 μM total surfactant (303 μM C20 components), which was close to the concentration where the adsorption plateau formed (200 μM C20 components, Figure 2B). The cmc of this postadsorption mixture was 310 $\pm$ 21 μM (232 μM C20 components) (Figure 5). This indicates that micelles started to form at the concentration where the adsorption plateau was reached and suggests that the occurrence of the plateau was indeed caused by formation of micelles.

The cmc of the postadsorption mixture was significantly higher than the cmc of the initial surfactant mixture, which was 148 $\pm$ 15 μM (114 μM C20 components) (Figure 5). The difference in cmc was presumably caused by the removal of the more hydrophobic components from the mixture by preferential adsorption. The dependence of the cmc of rhamnolipid mixtures on their composition is confirmed by the observation that the cmc of a separately produced rhamnolipid batch with lower amounts of C18 components and higher amounts of C22 components was reduced to 77 $\pm$ 6 μM (mole fractions for C18RL2, C18RL1, C20RL2, C20RL1, C22:1RL2, and C22RL2 were 0.04, 0.06, 0.57, 0.19, 0.08, and 0.05, respectively).

Column Studies. The adsorption of the multicomponent surfactant to Eustis soil and Borden aquifer material was also studied under continuous flow conditions using column experiments. The hydrodynamic properties of the columns were determined with pentafluorobenzoic acid as a conservative tracer. The breakthrough curves of this tracer were sigmoidal in shape and showed no tailing. Peclet numbers for the conservative tracer were greater than 100 for all columns. This indicates that physical nonequilibrium effects were absent and that the columns were packed homogeneously.

Breakthrough curves of total surfactant and of the individual components were determined for both soils using

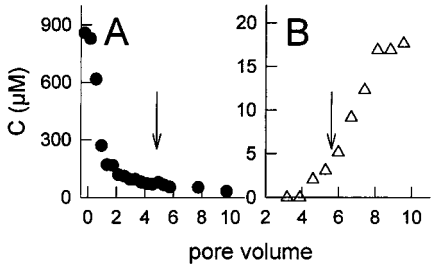

FIGURE 8. Effluent concentration of rhamnolipid during a flow-interrupted column experiment. (A) Distal limb of the breakthrough curve of total rhamnolipid in Borden soil. (B) Frontal limb of the breakthrough curve of C20RL2 in Eustis soil (△). The arrow indicates the time when the flow was interrupted for 8 h (A) or 1 h (B).

an influent concentration of 850 and 34 μM total surfactant (Figures 6 and 7). These concentrations were above and below the cmc of the surfactant, respectively. Breakthrough curves of total rhamnolipid were determined with surface tension measurements. In independent experiments, the breakthrough curves of the individual components were determined with HPLC-ELSD. The breakthrough curves of total surfactant were also calculated from the sum of the aqueous concentrations of the four major components in each effluent sample. These breakthrough curves matched the curves as obtained from surface tension measurements, indicating that the techniques were complementary. The retardation factors for the rhamnolipid components in Eustis soil were independent of the pore-water velocity for the velocities tested (15−100 cm/h).

To determine whether transport of rhamnolipid in soil columns was influenced by rate-limited adsorption, the flow was interrupted during breakthrough or during elution of rhamnolipid for a period ranging from 1 to 16 h (two examples shown in Figure 8). If nonequilibrium effects exist, a change in effluent concentration would be observed after interruption and subsequent recommencement of the flow (*24*). It was observed that changes in effluent concentration were absent for all components, at both influent concentrations and for both soils, indicating that transport of rhamnolipid was not affected by rate-limited adsorption.

The breakthrough curves of the individual rhamnolipids and of total rhamnolipid at both influent concentrations were characterized by a steep front and extended tailing in the distal part for both soils. A fast decrease in effluent concentration after elution with a rhamnolipid-free solution was observed especially at the supra-micellar influent concentration. For instance, the total surfactant concentration in the column effluent in experiments with an influent concentration of 850 μM became lower than 2 μM only after 200 or 70 pore volumes after rhamnolipid was no longer applied to the columns packed with Borden or Eustis soil, respectively. This extreme tailing could not be determined for the individual components because concentrations fell below the detection limit. Retardation factors for total surfactant and for all components were higher at $C_0 = 34$ μM than at 850 μM (Table 2). The transport behavior of rhamnolipid can be explained by the nonlinear (concave) adsorption isotherms of total rhamnolipid and of the individual components in the concentration range of the experiment.

Retardation factors for the C20 monorhamnolipid were higher than for the C20 dirhamnolipid for both soils and at both influent concentrations (Table 2). The retardation factors were also higher for the C20 components than for the C18 components (Table 2). These differences show that the components adsorbed to a different extent. This effect was most pronounced at the lowest value of C_0. As a result of differences in retardation between the components, the composition of the aqueous phase in the column effluent changed during breakthrough of the multicomponent surfactant.

TABLE 2. Retardation Factors for Total Surfactant and for Individual Components

		retardation factor[a]				
soil	C_0 (μM)	total surfactant	C18RL2	C18RL1	C20RL2	C20RL1
Borden	850	3.4	2.0	2.2	2.6	3.8
	34	7.0	4.7[b]	4.2[b]	6.3	8.0
Eustis	850	1.2	1.3	1.5	1.4	1.5
	34	ND[c]	4.0[b]	4.0[b]	10	17
Bonify	850	1.3[d]				
Vinton	850	1.9[d]				

[a] Determined from the area above the frontal limb of the breakthrough curve, unless mentioned otherwise. [b] From breakthrough time. [c] Not determined. [d] From ref 5.

Comparison of Surfactant Adsorption in Batch and Column Studies. The adsorbed concentration of the components in the column studies at full breakthrough was calculated from the retardation factors, using the formula $S_i = \theta/\rho(R-1)m_iC_0$, where S_i is the adsorbed concentration of component i and m_i is its mole fraction in the initial mixture. This concentration was compared to the adsorbed concentration that was observed at the same aqueous concentration of m_iC_0 of the same component during the batch experiments. At the supramicellar C_0 of 850 μM, the adsorbed concentration for all components was a factor 2 and 5 lower under continuous flow conditions than in the batch studies for Borden and Eustis, respectively. At $C_0 = 34$ μM, the difference was a factor 1−1.6 for all the components in both soils. The adsorbed surfactant concentration at a certain aqueous concentration may differ between column studies and batch experiments because adsorption of individual components in surfactants mixtures depends on the composition of the aqueous phase (*30*). The composition of the mobile phase at full breakthrough in column studies is different from the final composition in batch adsorption studies. The lower degree of surfactant adsorption in column experiments may also be attributed to the presence of shear stress during continuous flow conditions (*1*). Shear stress might counteract formation of surface aggregates and thereby reduce adsorption. This could be the reason for the larger difference between adsorption in batch and column experiments at higher C_0, since surface aggregates will be present mainly at the higher C_0.

Isotherm Shape. The observed isotherms of rhamnolipid adsorption to soil were composed of three regions: region I where sorption is determined by interactions between individual surfactants and soil, region II with a more pronounced increase of adsorbed concentration at increasing aqueous concentration due to secondary interactions between adsorbed surfactants, and an adsorption plateau. The results indicate that the formation of this adsorption plateau was caused by the onset of micellization. This implies that surfactant adsorption was determined by the concentration and composition of the monomeric surfactant (*2, 30*). The observed isotherm regions correspond to the regions I, II, and III described by Somasundaran and Krishnakumar (*31*) for adsorption of nonionic surfactants. The absence of an intermediate region between region II and III with a lower isotherm slope compared to region II (*31*) might indicate that electrostatic repulsion between the carboxylate moieties of rhamnolipid was low.

Surfactant Composition and cmc. The cmc of the postadsorption surfactant mixture was higher than the cmc of the initial mixture, which may be explained by preferential adsorption of hydrophobic components and enrichment of

the less hydrophobic components in the aqueous phase. The cmc of surfactant mixtures usually is determined by the individual cmc values of the components, by their mole fractions, and by their activity coefficients (*32*). Since the cmc of a surface active compound generally increases with decreasing hydrophobicity (*33, 34*), the critical micelle concentration of a surfactant mixture increases when the mixture is enriched in hydrophilic components.

Nature of the Adsorption Process. Adsorption of rhamnolipid to soils in region II and III was not primarily determined by the soil organic carbon content. For example, the amount of rhamnolipid adsorbed at the plateau region in the batch experiments was not dependent on the organic carbon content of the soils since the amount of surfactant adsorbed per amount of organic carbon differed 10-fold for Borden and Eustis soil, with values of 2.2 and 0.20 mg surfactant/mg organic matter, respectively. Similarly, the retardation factors for total rhamnolipid at $C_0 = 850\ \mu$M for the Borden material and Eustis soil (this study) and for Bonify and Vinton soil (*5*) were not correlated with the organic carbon content of these four soils (Table 2). Bonify and Vinton soil are sandy soils with an organic carbon content of 0.36% and 0.09%, respectively. The anionic character of the rhamnolipid surfactants might counteract partitioning into the negatively charged humic matter. Adsorption of an alcohol ethoxylate and alkylbenzene sulfonates to sediments was also not correlated to the soil organic carbon content (*35, 36*). In contrast, sorption of hydrophobic organic compounds to soil is often determined by the soil organic matter content and is therefore assumed to be a partitioning process instead of an adsorption process (*37*). Sorption of phenanthrene to the four soils mentioned here was indeed correlated to the soil organic matter content (*5*). These results imply that adsorption of rhamnolipid was an adsorption process occurring at the soil−water interface and not a partitioning process into soil organic matter. Primary interactions between the first adsorbed surfactant layer and soil might result from ion exchange reactions involving the anionic carboxylate moiety of the surfactant, surface complexation, or hydrogen bonding interactions involving the rhamnose headgroups (*31*).

Both in the batch and column studies, the adsorptivity of the components (defined as the percentage that was adsorbed) corresponded to the relative retention times of the (protonated) components in the isocratic reversed-phase HPLC system in the order of C18RL2 < C18RL1 < C20RL2 < C20RL1 (Figure 1, Table 1). The increase of adsorptivity of the components with increasing hydrophobicity suggests that adsorption of rhamnolipid components was driven by hydrophobic interactions. However, the lower mole fraction of C20RL1 than for C20RL2 in the initial mixture may also cause adsorption of C20RL1 to be relatively larger than for C20RL2 since the overall shapes of the isotherms were concave. A correlation between the degree of (preferential) adsorption of nonionic and anionic surfactant components and their hydrophobicity has also been observed for adsorption to soil (*9*) and to sediment (*35, 36*). Furthermore, hydrophobic interactions determined the concentration where region II started for isotherms adsorption nonionic surfactants on silica (*31, 34, 38*). Thermodynamic analysis of surfactant adsorption also indicates that hydrophobic interactions play an important role during adsorption of surfactants (*34, 39, 40*). The positive correlation of the adsorptivity of the rhamnolipid components with their hydrophobicity, and the absence of a positive correlation between the degree of adsorption and the soil organic matter content, suggests that adsorption of rhamnolipid to soil in regions II and III involved the formation of surface aggregates, such as hemimicelles or admicelles. These types of aggregates have been observed with AFM for adsorption of other surfactants containing two headgroups and two tails (gemini surfactants) (*17*).

The results from this study indicate that rhamnolipid adsorption to soil is an interfacial adsorption process which is driven by hydrophobic interactions between the rhamnolipid components. The adsorption of total surfactant and of the individual components increased with increasing total aqueous surfactant concentration up to a level where micelles started to form. Due to preferential adsorption, the composition of surfactant mixture remaining in the aqueous phase changed, both in the batch and column experiments. The changes in composition of the multicomponent surfactant due to adsorption affected the cmc of the surfactant mixture, and potentially also the solubilizing or emulsifying properties. To avoid the occurrence of changes of composition during application of mixed surfactants for enhanced oil recovery or soil remediation, high surfactant concentrations (≫cmc) should preferably be used. Due to the overall concave shape of the adsorption isotherms, both relative surfactant losses and changes in composition will then be minimal.

Acknowledgments

This research was funded by the Dutch IOP Environmental Biotechnology Program (Contract IOP91224). W.H.N. acknowledges the Dutch Program for Integrated Soil Research for a travelling grant (Project Number 35037-191).

Literature Cited

(1) Kwok, W.; Hayes, R. E.; Nasr-el-din, H. A. *Can. J. Chem. Eng.* **1995**, *73*, 705−716.
(2) Mannhardt, K.; Novosad, J. J. *Chem. Eng. Sci.* **1991**, *46*, 75−83.
(3) Jawitz, J. W.; Annable, M. D.; Rao, P. S. C.; Rhue, R. D. *Environ. Sci. Technol.* **1998**, *32*, 523−530.
(4) West, C. C.; Harwell, J. H. *Environ. Sci. Technol.* **1992**, *26*, 2324−2330.
(5) Noordman, W. H.; Ji, W.; Brusseau, M. L.; Janssen, D. B. *Environ. Sci. Technol.* **1998**, *32*, 1806−1812.
(6) Torrens, J. L.; Herman, D. C.; Miller, R. M. *Environ. Sci. Technol.* **1998**, *32*, 776−781.
(7) Edwards, D. A.; Adeel, Z.; Luthy, R. G. *Environ. Sci. Technol.* **1994**, *28*, 1550−1560.
(8) Nakae, A.; Tsuji, K.; Yamanaka, M. *Anal. Chem.* **1981**, *53*, 1818−1821.
(9) Kibbey, T. C. G.; Hayes, K. F. *Environ. Sci. Technol.* **1997**, *31*, 1171−1177.
(10) Passeri, A.; Lang, S.; Wagner, F.; Wray, V. *Z. Naturforsch. C* **1991**, *46*, 204−209.
(11) Kitamoto, D.; Yanagishita, H.; Shinbo, T.; Nakane, T.; Kamisawa, C.; Nakahara, T. *J. Biotechnol.* **1993**, *29*, 91−96.
(12) Jenny, K.; Kappeli, O.; Fiechter, A. *Appl. Microbiol. Biotechnol.* **1991**, *36*, 5−13.
(13) Rendell, N. B.; Taylor, G. W.; Somerville, M.; Todd, H.; Wilson, R.; Cole, P. J. *Biochim. Bioph. Acta* **1990**, *1045*, 189−193.
(14) Davila, A. M.; Marchal, R.; Monin, N.; Vandecasteele, J. P. *J. Chromatogr.* **1993**, *648*, 139−149.
(15) Van-Dyke, M. I.; Couture, P.; Brauer, M.; Lee, H.; Trevors, J. T. *Can. J. Microbiol.* **1993**, *39*, 1071−1078.
(16) Itoh, S.; Honda, H.; Tomita, F.; Suzuki, T. *J. Antibiot.* **1971**, *24*, 855−859.
(17) Manne, S.; Schäffer, T. E.; Huo, Q.; Hansma, P. K.; Morse, D. E.; Stucky, G. D.; Aksay, I. A. *Langmuir* **1997**, *13*, 6382−6387.
(18) Velikonja, J.; Kosaric, N. In *Biosurfactants*; Surfactant science series 48; Kosaric, N., Ed.; Marcel Dekker: New York, 1994; pp 419−446.
(19) Stanghellini, M. E.; Miller, R. M. *Plant Disease* **1997**, *81*, 4−12.
(20) Linhardt, R. J.; Bakhit, R.; Daniels, L.; Mayerl, F.; Pickenhagen, W. *Biotechnol. Bioeng.* **1989**, *33*, 365.
(21) Zhang, Y.; Miller, R. M. *Appl. Environ. Microbiol.* **1992**, *58*, 3276−3282.
(22) Rao, P. S. C.; Davidson, J. M.; Jessup, R. E.; Selim, H. M. *Soil Sci. Soc. Am. J.* **1979**, *43*, 22−28.
(23) Ball, W. P.; Roberts, P. V. *Environ. Sci. Technol.* **1991**, *25*, 1223−1237.
(24) Brusseau, M. L.; Rao, P. S. C.; Jessup, R. E.; Davidson, J. M. *J. Contam. Hydrol.* **1989**, *4*, 223−240.

(25) Chandrasekaran, E. V.; BeMiller, J. N. In *Methods in Carbohydrate Chemistry*; Whistler, R. L., BeMiller, J. N., Eds.; Academic Press: New York, 1980; Vol. 8, pp 89−96.
(26) Parker, J. C.; Van Genuchten, M. T. *Determining transport parameters from laboratory and field tracer experiments*; Bulletin 84-3; Virginia agricultural experiment station: Blacksburg, 1984.
(27) Arino, S.; Marchal, R.; Vandecasteele, J.-P. *Appl. Microbiol. Biotechnol.* **1996**, *45*, 162−168.
(28) Bear, G. R. *J. Chromatogr.* **1988**, *459*, 91−107.
(29) Lageveen, R. G.; Huisman, G. W.; Preusting, H.; Ketelaar, P.; Eggink, G.; Witholt, B. *Appl. Environ. Microbiol.* **1988**, *54*, 2924−2932.
(30) Trogus, F. J.; Schechter, R. S.; Wade, W. H. *J. Colloid Interface Sci.* **1979**, *70*, 293−305.
(31) Somasundaran, P.; Krishnakumar, S. *Colloids Surf. A* **1997**, *123−124*, 491−513.
(32) Nishikido, N. In *Surfactant science series*; Ogino, K., Abe, M., Eds.; Marcel Dekker: New York, 1993; Vol. 46, Mixed surfactant systems, pp 23−63.
(33) *Physicochemical properties of selected anionic, cationic, and nonionic surfactants*; Van Os, N. M., Haak, J. R., Rupert, L. A. M., Eds.; Elsevier: Amsterdam, 1993.
(34) Somasundaran, P.; Healy, T. W.; Fuerstenau, D. W. *J. Phys. Chem.* **1964**, *68*, 3562−3566.
(35) Cano, M. L.; Dorn, P. B. *Environ. Toxicol. Chem.* **1996**, *15*, 684−690.
(36) Hand, V. C.; Williams, G. K. *Environ. Sci. Technol.* **1987**, *21*, 370−373.
(37) Schwarzenbach, R. P.; Gschwend, P. M.; Imboden, D. M. *Environmental Organic Chemistry*, 1st ed.; John Wiley & Sons: New York, 1993.
(38) Portet, F.; Desbene, P. L.; Treiner, C. *J. Colloid Interface Sci.* **1996**, *184*, 216−226.
(39) Kronberg, B.; Costas, M.; Silveston, R. *Pure Appl. Chem* **1995**, *67*, 897−902.
(40) Mehrian, T.; De Keizer, A.; Korteweg, A. J.; Lyklema, J. *Colloids Surf. A* **1993**, *73*, 133−143.

Received for review August 30, 1999. Revised manuscript received December 3, 1999. Accepted December 7, 1999.

ES9909982